Letters

IOP Publishing

Plasma Sources Science and Technology

Plasma Sources Sci. Technol. **30** (2021) 10LT01 (6pp)

https://doi.org/10.1088/1361-6595/ac287b

Letter

Magnetic attenuation of the self-excitation of the plasma series resonance in low-pressure capacitively coupled discharges

Li Wang[1,2], Máté Vass[2,3], Zoltán Donkó[3], Peter Hartmann[3], Aranka Derzsi[3], Yuan-Hong Song[1,*] and Julian Schulze[1,2]

[1] Key Laboratory of Materials Modification by Laser, Ion, and Electron Beams (Ministry of Education), School of Physics, Dalian University of Technology, Dalian 116024, People's Republic of China

[2] Department of Electrical Engineering and Information Science, Ruhr-University Bochum, D-44780, Bochum, Germany

[3] Institute for Solid State Physics and Optics, Wigner Research Centre for Physics, H-1121 Budapest, Konkoly-Thege Miklós str. 29-33, Hungary

E-mail: songyh@dlut.edu.cn

Received 13 July 2021, revised 30 August 2021
Accepted for publication 20 September 2021
Published 8 October 2021

Abstract

External magnetic fields impose diverse effects on low-temperature plasmas. We study these in a low-pressure capacitively coupled radio frequency plasma in argon via self-consistent kinetic simulations. The primary effect of the transversal magnetic field, that manifests itself in the trapping of electrons at lower excitation frequencies and, thus, in an increase of the plasma density as a function of the magnetic field, is overruled at higher excitation frequencies by the attenuation of the self-excitation of plasma series resonance oscillations and the attenuation of non-linear electron resonance heating, which lead to a reduced plasma density. At higher magnetic fields the plasma density increases again due to (i) a longer interaction time between the electrons and the edges of the expanding sheaths and (ii) the electric field reversals that develop at the collapsing sheath edges to overcome the trapping of electrons and accelerate them towards the electrodes.

Keywords: capacitively coupled plasmas, plasma series resonance, attenuation of the self-excitation of the PSR

(Some figures may appear in colour only in the online journal)

Capacitively coupled plasma (CCP) sources are widely used in technological applications such as etching, deposition and sputtering due to their ability to generate large area and radially uniform plasmas [1–7]. With a static magnetic field applied to the system parallel to the electrodes, magnetized CCP sources are realized for applications such as magnetically enhanced reactive ion etching and are reported to provide improved plasma properties. In such plasma sources, higher plasma densities are obtained due to the enhanced

* Author to whom any correspondence should be addressed.

electron power absorption and reduced electron energy loss at the boundaries [8]. Typically, the plasma density increases monotonously as a function of the magnetic field [9, 10]. CCPs with more complex magnetic field topologies play an important role for other applications such as radio frequency (RF) sputtering [11–13]. For efficient knowledge based development and improvement of such applications of magnetized CCPs, a fundamental understanding of the effects of the magnetic field on the plasma, especially on the electron power absorption dynamics, is required. Investigations have been conducted by both experiments and simulations in recent years to explore the effects of the B-field on CCP discharge characteristics and plasma properties [13–21]. The magnetic asymmetry effect (MAE) [11, 22–24] was proposed and is considered to provide another way to control the discharge asymmetry in addition to the electrical asymmetry effect (EAE) [25–30] without changing the geometric reactor symmetry. Coupling effects between the MAE and geometric reactor asymmetries have been reported [11, 12].

At low pressure, plasma asymmetries have been found to cause high frequency oscillations of the RF current at frequencies higher than the applied RF due to the self-excitation of the plasma series resonance (PSR) [31–38]. By analyzing the spatio-temporal electron dynamics, Wilczek *et al* [39] explained the kinetic origin of the PSR using Particle-in-Cell/Monte-Carlo collisions (PIC/MCC) simulations. These findings have been verified experimentally by Berger *et al* [40]. The continuous interaction of bulk electrons with the expanding sheath via the self-excitation of PSR strongly enhances the electron power absorption via nonlinear electron resonance heating (NERH) [33]. These kinetic mechanisms are found to occur at low pressures in asymmetric CCPs as well as symmetric CCPs with high driving frequencies, where the sheath expansion velocity is fast and a strong PSR is excited. At high pressures these oscillations are damped by collisions.

Previous studies revealed that the self-excitation of the PSR can be controlled via the EAE. Donkó *et al* [37] reported that by tuning the phase angle between two consecutive harmonics of a dual-frequency driving voltage waveform, the PSR and NERH can be turned on and off. The self-excitation of the PSR can be moved from one electrode to the other by phase control. Recently, it has been demonstrated that, similar to the EAE, the MAE can also control the self-excitation of the PSR by adjusting a non-uniform magnetic field [12, 41, 42]. Oberberg *et al* [12, 41] found that the PSR is strongly excited near the smaller powered electrode in an unmagnetized geometrically asymmetric system. By increasing the magnetic field near the powered electrode, while keeping the B-field low at the grounded electrode, the geometrical asymmetry can be compensated by the magnetic asymmetry. The discharge becomes symmetric and no PSR is excited. With further increasing the B-field, the asymmetry of the discharge is inverted and the self-excitation of the PSR shifts to the grounded electrode.

Such studies have shown strong effects of non-uniform externally applied magnetic fields on the PSR self-excitation via adjusting the symmetry of the CCP discharge. In this work, we demonstrate that the PSR excitation is also greatly affected by uniform transversal B-fields in magnetically symmetric systems where a homogeneous magnetic field is applied parallel to the electrodes and the discharge symmetry remains unchanged. Our simulation results show that PSR oscillations of the RF current are self-excited at high driving frequencies (60 MHz) in unmagnetized geometrically symmetric low pressure discharges. Applying a uniform external B-field parallel to the electrodes is found to cause a strong attenuation of the self-excitation of these PSR oscillations as a function of the magnetic field strength at low magnetic fields, which leads to a significant reduction of the NERH and of the space averaged plasma density. At higher B-fields, the plasma density increases again due to the enhanced magnetic electron confinement. Such effects are studied in detail in this work by using PIC/MCC simulations. These effects of the B-field are markedly different compared to those observed in magnetically asymmetric CCPs, where a non-uniform magnetic field affects the plasma symmetry and was found to enhance the self-excitation of the PSR. Here, the opposite effect of the B-field on the PSR is observed, i.e. an attenuation of the self-excitation of the PSR induced by the B-field.

We conduct 1d3v (one-dimensional in space and three-dimensional in velocity space) electrostatic PIC/MCC simulations of a geometrically symmetric CCP in argon. As shown in figure 1, the plasma is operated between two plane parallel electrodes separated by a gap of $L = 2.5$ cm with the top electrode ($x = L$) grounded and the bottom electrode ($x = 0$) driven by a single-frequency voltage waveform at $f = 60$ MHz with a voltage amplitude of $V_0 = 300$ V. An axially homogeneous magnetic field is applied parallel to the electrodes. In the simulations, the electrons as well as Ar^+ ions are traced. The gas temperature is fixed at 350 K, the pressure is set to $p = 10$ mTorr. The ion induced secondary electron emission and electron reflection coefficients at the boundaries are 0.07 and 0.7, respectively, representing a simple model for stainless steel [43]. The time step is 5.6×10^{-12} s; the grid size is set to 3.125×10^{-5} m to fulfil all stability criteria of the PIC/MCC method. The superparticle number ranges from 5×10^5 to 5.5×10^5. The original PIC/MCC code (without external magnetic field and with different ion cross sections compared to the code used in this work) was used in several previous works [44–47] and has been verified by experiments to be reliable [48]. In case of a magnetic field included, the code was benchmarked against simulation results in [49]. In the present work, the ion cross sections are updated [50], by which the collision processes and cross sections considered are the same as those in [51]. By comparing the results obtained with this code to those presented in [51], good agreement was achieved.

Figure 2 shows the time-averaged electron density profiles at different externally applied transversal magnetic fields of $B = 0$ G, 20 G, 40 G and 80 G. The gap distance, neutral gas pressure, driving voltage amplitude and frequency are kept constant at $L = 2.5$ cm, $p = 10$ mTorr, $V_0 = 300$ V, and $f = 60$ MHz, respectively. Previous works have shown that the electron density increases monotonously as a function of the magnetic field at low frequencies, e.g. 13.56 MHz, which is ultimately caused by the enhanced electron confinement at

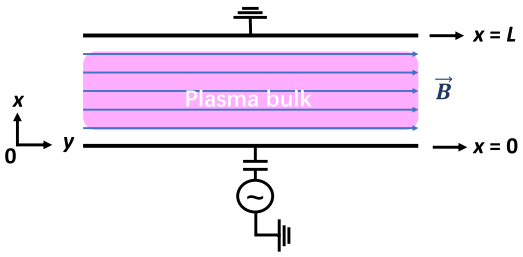

Figure 1. Schematic of a symmetric capacitive RF discharge in the presence of a uniform magnetic field parallel to the electrodes.

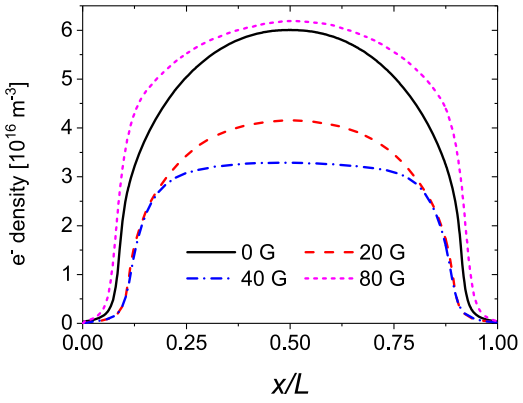

Figure 2. Time-averaged electron density profile at $B = 0$ G, 20 G, 40 G and 80 G. Other discharge conditions: $L = 2.5$ cm, $p = 10$ mTorr, $V_0 = 300$ V, and $f = 60$ MHz.

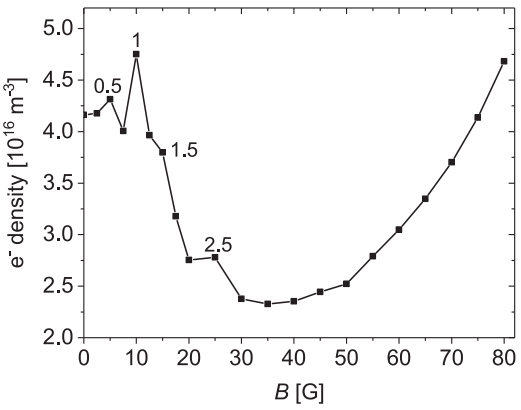

Figure 3. Space- and time-averaged electron density as a function of the magnitude of the parallel and uniform magnetic field at $f = 60$ MHz. Other discharge conditions: $L = 2.5$ cm, $p = 10$ mTorr, and $V_0 = 300$ V. The small peaks at low magnetic fields are labeled by numbers that correspond to the approximate ratio $2f_{ce}/f$.

higher magnetic fields [9, 10]. Our results indicate that this is not the case at higher driving frequencies such as 60 MHz. The electron density is found to decrease as a function of the magnetic field at low field strength ranging from 0 to 40 G. Its peak value drops from nearly 6×10^{16} m^{-3} at 0 G to about 3×10^{16} m^{-3} at 40 G. Beyond 40 G the plasma density increases as a function of the B-field (similar to low-frequency CCPs) and reaches a value of about 6×10^{16} m^{-3} at 80 G. As a result of the changed plasma density, the sheath width also varies as a function of the magnetic field, i.e. the sheath widths are 0.22 cm, 0.28 cm, 0.28 cm and 0.19 cm at $B = 0$ G, 20 G, 40 G, and 80 G, respectively.

The influence of the external magnetic field on the space- and time-averaged plasma density at 60 MHz is shown in figure 3. While the electron density increases monotonously with enhancing the magnetic field at low frequencies, its dependence on the magnetic field is very different at high frequencies, i.e. the electron density decreases initially and then gradually increases with the B-field. This behaviour of the electron density as a function of the magnetic field is correlated with the presence/absence of self-excited high frequency PSR oscillations of the RF current and, thus, NERH as will be shown in the following. In addition to these general trends, small peaks of the plasma density are observed at 5 G, 10 G and 25 G. These are caused by the Magnetic Sheath Resonance recently proposed by Zhang *et al* and Patil *et al* [52, 53]. At these specific magnetic fields a synchronization of the sheath oscillation and the electron cyclotron motion happens, i.e. an electron accelerated into the plasma bulk by the expanding sheath is returned to the sheath by its gyro-motion around the magnetic field lines, when the sheath is expanding again. The corresponding density maxima in figure 3 are labeled by numbers that correspond to the approximate ratio $2f_{ce}/f$, where f_{ce} is the electron cyclotron resonance frequency and f is the driving frequency. Via this magnetic sheath resonance the electron power absorption and, thus, the plasma density are enhanced at distinct magnetic field strengths.

Figure 4 shows the total current density as a function of time within one RF period and its Fourier spectrum at $f = 60$ MHz for different magnetic field strengths of $B = 0$ G, 20 G, 40 G and 80 G. PSR oscillations are observed at 0 G and the corresponding higher harmonic components (at around 10×60 MHz) appear in the Fourier spectrum. At 20 G, the self-excitation of the oscillations starts to be attenuated. At higher B-fields, i.e. 40 G and 80 G, the self-excitation of high frequency PSR oscillations is attenuated even further due to the magnetic field effect. Consequently, the NERH is also attenuated as a function of the externally applied magnetic field. As discussed in the work of Wilczek *et al* [39], such PSR oscillations of the RF current are self-excited in unmagnetized high frequency discharges at $B = 0$ G. Consequently, the electron power absorption is significantly enhanced by NERH, which results in high plasma densities. A magnetic field applied to the discharge, i.e. $B > 0$ G, attenuates the self-excitation of the PSR oscillations and reduces the NERH, which leads to a decreased electron density at moderate externally applied magnetic fields. At higher magnetic fields the electron density increases again as a function of the externally applied B-field similar to the low-frequency cases. As discussed in previous studies [10], the enhanced electron density at high B-fields is mainly caused by the following effects: the electron interaction time with the expanding sheaths is extended, the electron power absorption is enhanced by magnetically induced electric field reversals during the sheath collapses, and the electron energy loss at the boundaries is reduced by increasing the B-field, i.e. electrons

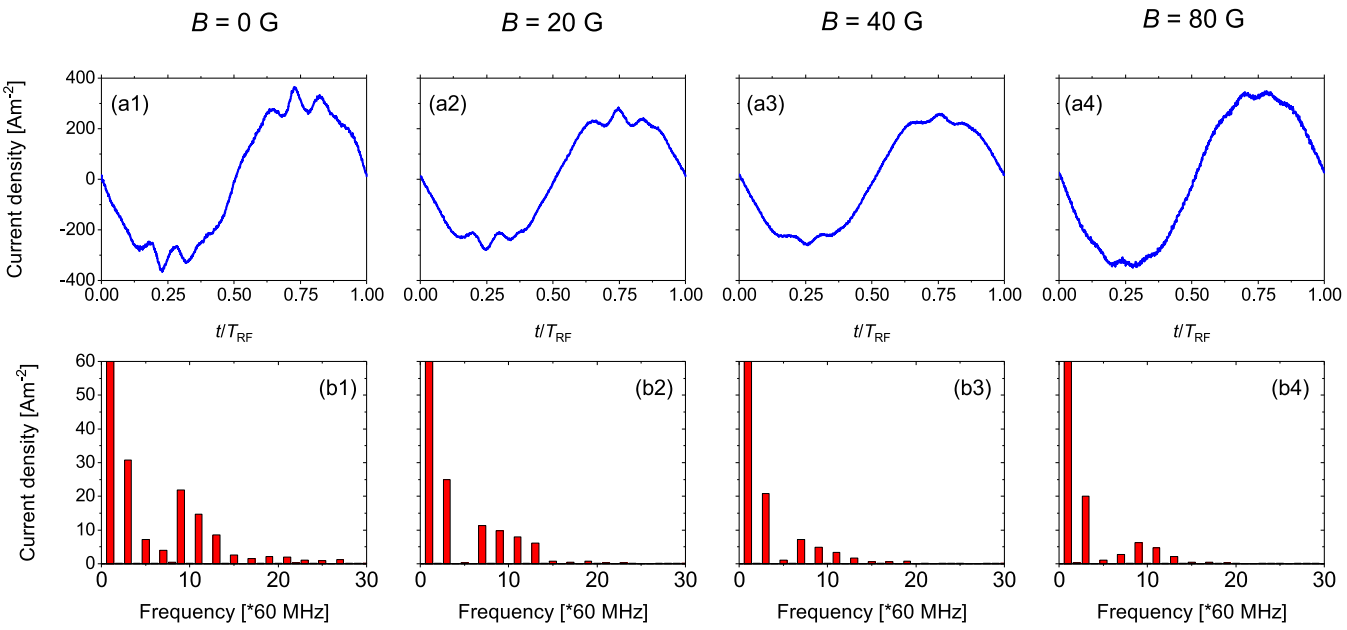

Figure 4. Total current density as a function of time within one RF period at the discharge center for different magnetic field strengths (first row) and the corresponding Fourier spectra (second row) at $f = 60$ MHz. The range of the vertical axes in the second row is chosen to make the changes at the higher harmonics more visible. The amplitude values of the first harmonic are 334, 266, 260, and 356 Am^{-2} for 0, 20, 40, and 80 G, respectively, which cannot be seen in the figure. Other discharge conditions: $L = 2.5$ cm, $p = 10$ mTorr, and $V_0 = 300$ V.

experience more collisions before they are lost at the electrodes. In the Fourier spectrum plots, some lower harmonics (3×60 MHz and 5×60 MHz) are also observed. As shown in previous studies [31, 33], these harmonics are not induced by the PSR, but generally exist in the discharge even without the excitation of the PSR. At high B-fields, these harmonics are also attenuated, since the electrons are well confined by the magnetic field and their ability of instantaneous response is weakened.

We note that some dependence of the electron density as a function of the superparticle number is observed in our simulations. This is a well known effect in PIC/MCC simulations [54, 55]. With the presence of the PSR, such variations of the electron density lead to small changes of the PSR frequencies. In order to minimize such effects we keep the superparticle number approximately constant for all values of the magnetic field studied in this work. The main effect observed here, i.e. the magnetic attenuation of the self-excitation of the PSR and the related reduction of the plasma density as a function of the B-field at low field strength, is not affected by this phenomenon.

Spatio-temporal plots of the electric field, the electron heating rate, and the ionization rate at $B = 0$, 20, 40, and 80 G are shown in figure 5. Strong PSR oscillations are found to be excited at $B = 0$ G, which lead to the generation of energetic electron beams and to a high electron power absorption rate during the sheath expansion caused by NERH. As the pressure is low, the energetic electron beams generated by sheath expansion heating can penetrate far into the bulk region and lead to strong ionization there, as shown in figure 5(c1). At $B = 20$ G, NERH is significantly attenuated as shown in figure 5(b2), which leads to a lower ionization rate near the expanding sheaths and finally results in a reduced plasma density. The lower NERH is caused by the magnetic attenuation of the self-excitation of the PSR. The PSR is self-excited kinetically due to a fast sheath expansion in combination with electron inertia [39]. The quick sheath expansion leads to a compression of electrons at the expanding sheath edge and the generation of an initial beam of energetic electrons that propagates into the plasma bulk. A positive space charge is left behind on the bulk side of the expanding sheath edge due to the flux of these electrons away from the sheath edge. This positive space charge pulls cold bulk electrons towards the sheath, which upon interaction with the expanding sheath edge form the next energetic electron beam and the previously described process starts again. With a magnetic field applied parallel to the electrodes, the beam electrons are confined more strongly near the sheath, i.e. at high B-fields they cannot propagate away from the expanding sheath edge and, thus, no positive space charge is left behind that attracts bulk electrons. The self-excitation of the PSR is, thus, attenuated magnetically. This magnetic attenuation of the self-excitation of the PSR is different from collisional damping of the PSR in unmagnetized CCPs at higher pressures in the sense that the electrons lose energy in collisions, whereas in case of the magnetic effect their energy is not lost, but their direction of motion is changed.

At 40 G, the higher B-field enhances the electron power absorption during the sheath expansion phase by confining the electrons near the sheath edge and extending their interaction time with the expanding sheath. However, the self-excitation of the PSR is further attenuated, which further reduces the NERH. Most of the ionization occurs near the sheath edges since the energetic electrons cannot penetrate far into the bulk region due the confinement by the B-field. As illustrated by the density profiles in figure 2, the electron density is lower at 40 G compared to the 20 G case. At 80 G the NERH has

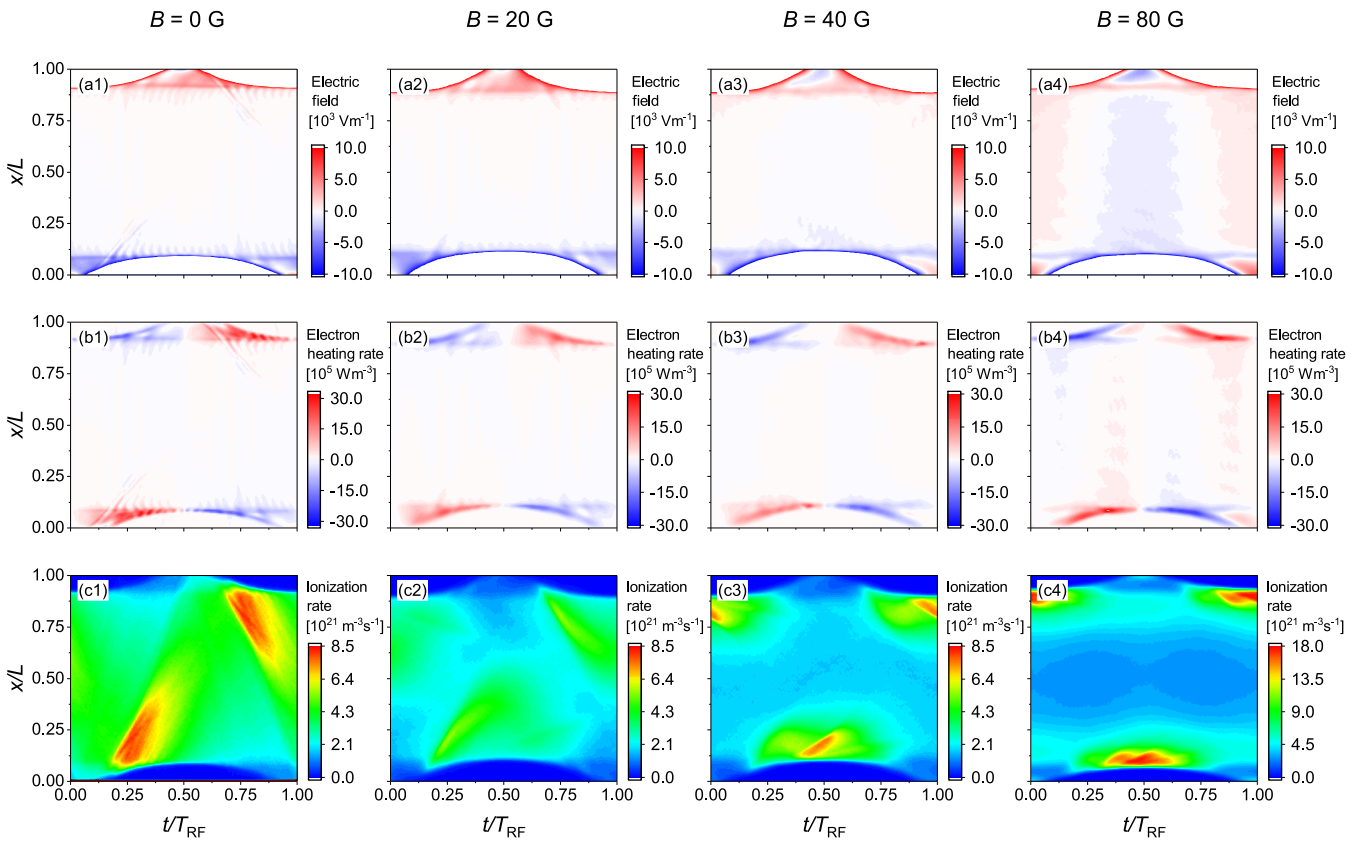

Figure 5. Spatio-temporal plots of the electric field (first row), the electron heating rate (second row), and the ionization rate (third row) at $B = 0, 20, 40$ and 60 G at $f = 60$ MHz. Other discharge conditions: $L = 2.5$ cm, $p = 10$ mTorr, and $V_0 = 300$ V.

almost disappeared, while the total electron power absorption is enhanced strongly, which leads to an increase of the electron density. The enhanced electron power absorption at high magnetic fields is caused by the mechanisms mentioned above, i.e. the B-field enhances the interaction of electrons with the expanding sheaths and reduces the electron energy loss at the electrodes. Meanwhile, a strong electric field reversal is generated during the sheath collapse, which also contributes to the electron power absorption [10]. We notice that due to the low conductivity, a drift electric field in the bulk region is evident, which is strongest shortly before each sheath expands to its maximum width.

In conclusion, using 1d3v PIC/MCC simulations, the effects of a uniform transversal magnetic field on high-frequency capacitively coupled discharges were studied. In unmagnetized discharges, high-frequency PSR oscillations of the RF current are found to be self-excited and to enhance the electron power absorption by NERH. With a transversal B-field applied, the transport of the electrons perpendicular to the electrodes is reduced, which leads to an attenuation of the self-excitation of PSR oscillations. This effect reduces the plasma density and leads to a different dependence of the plasma density on the magnetic field strength as compared to low-frequency discharges, since the NERH is attenuated by the weakened self-excitation of the PSR and the electron density is reduced as a function of the magnetic field at low B-fields. Further increasing the B-field, the electron density increases as a function of the magnetic field, since the enhancement mechanisms of the electron power absorption dominate. The magnetic attenuation of the self-excitation of the PSR is important for the fundamental understanding of magnetized CCPs and for the knowledge based plasma process development for various industrial applications. In asymmetric low-pressure CCPs, the PSR is self-excited more strongly and, thus, even stronger effects of the magnetic field are expected in such reactors.

Acknowledgments

This work was supported by the National Natural Science Foundation of China (Nos. 12020101005, 11975067), China Scholarship Council (201906060024), by the German Research Foundation in the frame of the project 'Plasmabasierte Prozessfüuhrung von reaktiven Sputterprozessen' (No. 417888799), and the project 'Electron heating in capacitive RF plasmas based on moments of the Boltzmann equation: from fundamental understanding to knowledge based process control' (No. 428942393), by the National Office for Research, Development and Innovation of Hungary (NKFIH) via Grants K-134462, K-132158, FK-128924.

Data availability statement

The data that support the findings of this study are available upon reasonable request from the authors.

ORCID iDs

Li Wang https://orcid.org/0000-0002-3106-2779
Máté Vass https://orcid.org/0000-0001-9865-4982
Zoltán Donkó https://orcid.org/0000-0003-1369-6150
Peter Hartmann https://orcid.org/0000-0003-3572-1310
Aranka Derzsi https://orcid.org/0000-0002-8005-5348
Yuan-Hong Song https://orcid.org/0000-0001-5712-9241
Julian Schulze https://orcid.org/0000-0001-7929-5734

References

[1] Lieberman M A and Lichtenberg A J 2005 *Principles of Plasma Discharges and Materials Processing* 2nd edn (New York: Wiley)
[2] Makabe T and Petrovic Z L 2014 *Plasma Electronics: Applications in Microelectronic Device Fabrication* 2nd edn (Boca Raton, FL: CRC Press)
[3] Chabert P and Braithwaite N 2011 *Physics of Radio-Frequency Plasmas* (Cambridge: Cambridge University Press)
[4] Huang S, Huard C, Shim S, Nam S K, Song I-C, Lu S and Kushner M J 2019 *J. Vac. Sci. Technol.* A **37** 031304
[5] Zhang Y, Kushner M J, Sriraman S, Marakhtanov A, Holland J and Paterson A 2015 *J. Vac. Sci. Technol.* A **33** 031302
[6] Wilczek S, Schulze J, Brinkmann R P, Donkó Z, Trieschmann J and Mussenbrock T 2020 *J. Appl. Phys.* **127** 181101
[7] Makabe T 2019 *Japan J. Appl. Phys.* **58** 110101
[8] Kushner M J 2003 *J. Appl. Phys.* **94** 1436–47
[9] Yang S, Zhang Y, Wang H-Y, Wang S and Jiang W 2017 *Phys. Plasmas* **24** 033504
[10] Wang L, Wen D-Q, Hartmann P, Donkó Z, Derzsi A, Wang X-F, Song Y-H, Wang Y-N and Schulze J 2020 *Plasma Sources Sci. Technol.* **29** 105004
[11] Oberberg M, Kallähn J, Awakowicz P and Schulze J 2018 *Plasma Sources Sci. Technol.* **27** 105018
[12] Oberberg M *et al* 2020 *Plasma Sources Sci. Technol.* **29** 075013
[13] Zheng B, Fu Y, Wang K, Schuelke T and Fan Q H 2021 *Plasma Sources Sci. Technol.* **30** 035019
[14] Zheng B, Wang K, Grotjohn T, Schuelke T and Fan Q H 2019 *Plasma Sources Sci. Technol.* **28** 09LT03
[15] Gerst D, Cuynet S, Cirisan M and Mazouffre S 2013 *Plasma Sources Sci. Technol.* **22** 015024
[16] Lieberman M A, Lichtenberg A J and Savas S E 1991 *IEEE Trans. Plasma Sci.* **19** 189–96
[17] Bera K, Rauf S, Kenney J, Dorf L and Collins K 2010 *J. Appl. Phys.* **107** 053302
[18] Lee S H, You S J, Chang H Y and Lee J K 2007 *J. Vac. Sci. Technol.* A **25** 455–63
[19] Benyoucef D and Yousfi M 2015 *Phys. Plasmas* **22** 013510
[20] You S J, Chung C W, Bai K H and Chang H Y 2002 *Appl. Phys. Lett.* **81** 2529–31
[21] Turner M M, Hutchinson D A W, Doyle R A and Hopkins M B 1996 *Phys. Rev. Lett.* **76** 2069–72
[22] Trieschmann J, Shihab M, Szeremley D, Elgendy A E, Gallian S, Eremin D, Brinkmann R P and Mussenbrock T 2013 *J. Phys. D: Appl. Phys.* **46** 084016
[23] Yang S, Zhang Y, Wang H, Cui J and Jiang W 2017 *Plasma Process Polym.* **14** 1700087
[24] Yang S, Chang L, Zhang Y and Jiang W 2018 *Plasma Sources Sci. Technol.* **27** 035008
[25] Donkó Z, Schulze J, Heil B G and Czarnetzki U 2008 *J. Phys. D: Appl. Phys.* **42** 025205
[26] Schulze J, Schüngel E, Donkó Z and Czarnetzki U 2011 *Plasma Sources Sci. Technol.* **20** 015017
[27] Schulze J, Schüngel E, Donkó Z and Czarnetzki U 2010 *Plasma Sources Sci. Technol.* **19** 045028
[28] Brandt S *et al* 2016 *Plasma Sources Sci. Technol.* **25** 045015
[29] Lafleur T 2015 *Plasma Sources Sci. Technol.* **25** 013001
[30] Lafleur T, Delattre P A, Johnson E V and Booth J P 2012 *Appl. Phys. Lett.* **101** 124104
[31] Czarnetzki U, Mussenbrock T and Brinkmann R P 2006 *Phys. Plasmas* **13** 123503
[32] Schulze J, Heil B G, Luggenhölscher D, Brinkmann R P and Czarnetzki U 2008 *J. Phys. D: Appl. Phys.* **41** 195212
[33] Mussenbrock T, Brinkmann R P, Lieberman M A, Lichtenberg A J and Kawamura E 2008 *Phys. Rev. Lett.* **101** 085004
[34] Wen D-Q, Kawamura E, Lieberman M A, Lichtenberg A J and Wang Y-N 2016 *Plasma Sources Sci. Technol.* **26** 015007
[35] Schulze J, Heil B G, Luggenholscher D and Czarnetzki U 2008 *IEEE Trans. Plasma Sci.* **36** 1400–1
[36] Schulze J, Heil B G, Luggenhölscher D, Mussenbrock T, Brinkmann R P and Czarnetzki U 2008 *J. Phys. D: Appl. Phys.* **41** 042003
[37] Donkó Z, Schulze J, Czarnetzki U and Luggenhölscher D 2009 *Appl. Phys. Lett.* **94** 131501
[38] Schüngel E, Brandt S, Donkó Z, Korolov I, Derzsi A and Schulze J 2015 *Plasma Sources Sci. Technol.* **24** 044009
[39] Wilczek S *et al* 2016 *Phys. Plasmas* **23** 063514
[40] Berger B, You K, Lee H-C, Mussenbrock T, Awakowicz P and Schulze J 2018 *Plasma Sources Sci. Technol.* **27** 12LT02
[41] Oberberg M, Engel D, Berger B, Wölfel C, Eremin D, Lunze J, Brinkmann R P, Awakowicz P and Schulze J 2019 *Plasma Sources Sci. Technol.* **28** 115021
[42] Liu Y, Trieschmann J, Berger B, Schulze J and Mussenbrock T 2021 *Phys. Plasmas* **28** 053505
[43] Schulenberg D A *et al* 2020 *Plasma Sources Sci. Technol.* accepted (https://doi.org/10.1088/1361-6595/ac2222)
[44] Jiang W, Xu X, Dai Z-L and Wang Y-N 2008 *Phys. Plasmas* **15** 033502
[45] Jiang W, Wang H-y, Zhao S-x and Wang Y-n 2009 *J. Phys. D: Appl. Phys.* **42** 102005
[46] Zhang Q-Z, Jiang W, Zhao S-X and Wang Y-N 2010 *J. Vac. Sci. Technol.* A **28** 287–92
[47] Zhang Q-Z, Liu Y-X, Jiang W, Bogaerts A and Wang Y-N 2013 *Plasma Sources Sci. Technol.* **22** 025014
[48] Liu Y X, Zhang Q Z, Jiang W, Hou L J, Jiang X Z, Lu W Q and Wang Y N 2011 *Phys. Rev. Lett.* **107** 055002
[49] Yang S, Zhang Y, Wang H-Y, Wang S and Jiang W 2017 *Plasma Sources Sci. Technol.* **26** 065011
[50] Phelps A V 1994 *J. Appl. Phys.* **76** 747–53
[51] Donkó Z, Derzsi A, Vass M, Horváth B, Wilczek S, Hartmann B and Hartmann P 2021 *Plasma Sources Sci. Technol.* **30** 095017
[52] Zhang Q Z *et al* 2020 *Phys. Rev.* E accepted (https://journals.aps.org/pre/accepted/9007aY2bKcc1c27e617e3329676337b522f4bebb1)
[53] Patil S, Sharma S, Sengupta S, Sen A and Kaganovich I 2020 An enhanced operating regime for high frequency capacitive discharges (arXiv:2012.02752)
[54] Turner M M 2006 *Phys. Plasmas* **13** 033506
[55] Erden E and Rafatov I 2014 *Contrib. Plasma Phys.* **54** 626–34